

Changes in the state of iron atoms in Zr alloys during corrosion tests in an autoclave

V. P. Filippov · A. B. Bateev · Yu. A. Lauer ·
N. I. Kargin · V. I. Petrov

© Springer Science+Business Media Dordrecht 2013

Abstract Mössbauer investigations were carried out on oxide films formed on specimens of zirconium alloys Zr-1.0 %wtFe-1.2 %wtSn-0.5 %wtCr subjected to corrosion in steam-water environment at a temperature of 360 °C and at a pressure of 16.8 MPa with lithium and boron additions, and on Zr-1.4 %wtFe-0.7 %wtCr corroded in steam-water environment at 350 °C and 16.8 MPa as well as in steam-water environment at 500 °C and 10 MPa. In the metal part of the samples, under the oxide film, the iron atoms are in form of intermetallic precipitates of $Zr(Fe, Cr)_2$. The corrosion process decomposes the intermetallic precipitates and particles are formed of metallic iron with inclusions of chromium atoms –Fe(Cr), α -Fe₂O₃ and Fe₃O₄ compounds. Part of the iron ions are in divalent and part in trivalent paramagnetic states. It is proposed that some part of the iron containing oxide precipitates in the oxide film may be in the form of nanoparticles which pass from the superparamagnetic to the ferromagnetic state with decreasing temperature.

Keywords Mössbauer effect · Zirconium alloys · Intermetallic precipitates · Oxide film · Superparamagnetic particles

1 Introduction

The development of nuclear power plants goes in the direction of increasing safety of the power station together with increasing the lifetime of tubes by 6–7 years and increasing the burning out of fuel till 60–70 MWdays/kgU. The solution of this problem is partially connected with the improvement of the corrosion resistance of zirconium alloys. The knowledge of the state and the redistribution of atoms in the alloying elements is necessary for

Proceedings of the 32nd International Conference on the Applications of the Mössbauer Effect (ICAME 2013) held in Opatija, Croatia, 1–6 September 2013

V. P. Filippov (✉) · A. B. Bateev · Yu. A. Lauer · N. I. Kargin · V. I. Petrov
National Research Nuclear University “MEPhI”, Moscow, Russia
e-mail: vpfilippov@mephi.ru

understanding the corrosion process of zirconium alloys and the formation of oxide films, in particular for iron atoms that can be incorporated in nanoparticles.

In this paper oxide films formed on samples of zirconium alloys (1) Zr-1.0 wt%Fe-1.2 wt%Sn-0.5 wt%Cr in steam-water environment with lithium and boron additions at temperature $t = 360\text{ }^{\circ}\text{C}$ and pressure $p = 16.8\text{ MPa}$ and (2) Zr-1.4 wt%Fe-0.7 wt% Cr in steam-water environment at $t = 350\text{ }^{\circ}\text{C}$ and $p = 16.8\text{ MPa}$ and in steam environment at $t = 500\text{ }^{\circ}\text{C}$ and $p = 10\text{ MPa}$ were investigated by the help of Mössbauer spectroscopy.

2 Experimental

Zirconium has no resonant isotopes for carrying out Mössbauer research, but industrial zirconium alloys (Zircaloy-2, E635) contain iron as alloying element. For the present investigations alloys were prepared from zirconium of nuclear purity by adding pure iron, tin and chromium as alloying elements. Iron and tin were enriched with ^{57}Fe and ^{119}Sn . The alloys were melted in an arc furnace using a W electrode in clean argon atmosphere. The remeltings were carried out not less than five times. The composition of the alloys was determined by chemical analysis. Then the melted samples of the alloys were forged, hot rolled in a copper cover at $750\text{ }^{\circ}\text{C}$ till 2.7 mm thickness and then cold rolled [1].

Before the corrosion tests samples with size $10 \times 20 \times 0.8\text{ mm}^3$ were cut out along the rolling direction. Then they were mechanically polished achieving a roughness of no more than $0.6\text{ }\mu\text{m}$. The samples were exposed to a homogenization and subjected to an annealing in dynamic vacuum not worse than $7 \cdot 10^{-4}\text{ Pa}$ and were polished chemically in a solution of HF and nitric acids. These samples were exposed to corrosion tests. Corrosion tests were carried out in an autoclave prepared from stainless steel and filled with distilled water.

The thickness of the zirconium dioxide was determined by additional weighting. It was assumed that all oxygen participates in the formation of the oxide film with equal density of zirconia of monoclinic structure.

In earlier studies the oxide surface film was separated by dissolution of the metal substrate in a 3 % solution of fluoric acid. This process can lead to a mixture of the remaining oxide film with products of the chemical reaction. In the present work the oxide film was separated mechanically from the alloy sample. The samples for Mössbauer measurements were prepared from such separated films. Mössbauer measurements were carried out with spectrometers operating in constant velocity mode as well as in acceleration mode, with a source of $^{57}\text{Co}(\text{Cr})$. Spectra of the oxide samples as well of etalon samples of metallic α -iron and compounds $\alpha\text{-Fe}_2\text{O}_3$ and Fe_3O_4 , were obtained at different temperatures ($T = 298\text{ K}$, $T = 80\text{ K}$) for a more exact identification of iron containing phases.

3 Results and discussion

3.1 State of iron in alloys

The ^{57}Fe spectra of the alloy (1) are presented in Figs. 1 and 2. The spectrum evaluation of alloy (1) in Fig. 1 shows the occurrence of intermetallic compounds $\text{Zr}(\text{Fe},\text{Cr})_2^{\text{I}}$ (cubic C15), $\text{Zr}(\text{Fe},\text{Cr})_2^{\text{II}}$ (hexagonal C14) [1, 2] and Zr_3Fe [3, 4]. The quantity of Zr_3Fe on the surface of the sample is larger than inside the sample. Figure 1 shows that the relative intensity of the lines corresponding to Zr_3Fe is larger in the CEM spectrum (Fig. 1b) than in the transmission spectrum (Fig. 1a).

Fig. 1 ^{57}Fe spectra of alloy Zr-1.0 wt%Fe-1.2 wt%Sn-0.5 wt%Cr: (a) transmission geometry, (b) CEM. The spectra are obtained at room temperature

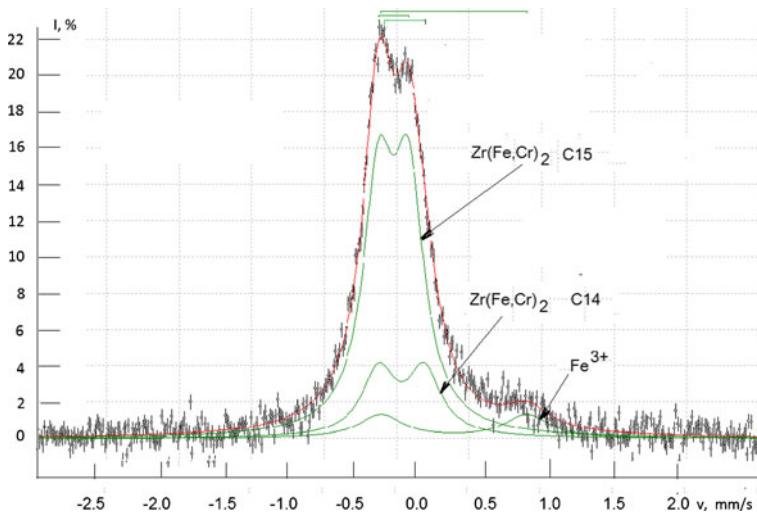
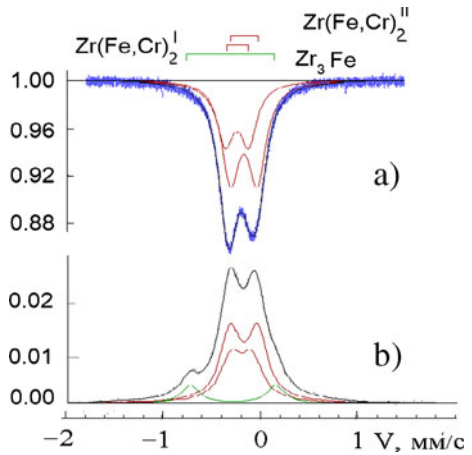


Fig. 2 The spectrum of the metallic part of alloy (2) sample obtained after removal of an oxide film with a thickness of $14.0\ \mu\text{m}$ from the specimen after 2390 h of corrosion

The same phases are identified in samples of alloy 2. It is interesting to know the state of iron on the surface of the alloys under the oxide film. Figure 2 shows the CEM spectrum of ^{57}Fe on the surface of the sample obtained after removal of an oxide film with a thickness of $14.0\ \mu\text{m}$ from the sample after 2390 h of corrosion. The spectrum was obtained at room temperature.

The analysis of spectrum shows the existence of several doublets with quadrupole splitting parameters similar to the ones of the intermetallic compound $\text{Zr}(\text{Fe}_{1-x}\text{Cr}_x)_2$ (types C14, C15). The presence of a doublet with parameters $QS = 1.2 \pm 0.1\ \text{mm/s}$ and $IS = 0.37 \pm 0.05\ \text{mm/s}$ is explained by the occurrence of unremoved oxide on the surface, assigned to the solid solution of Fe^{3+} in ZrO_2 [5]. Because the oxide film was separated mechanically a certain fraction of the underlying metal should be present in this our oxide

sample. So in the central part of spectrum of the separated oxide film could be the lines of intermetallic precipitates.

The comparison of the evolutions of the obtained spectra of the alloys (1 and 2) with different composition shows that there is no significant influence of Sn on state of iron in the alloys.

The presence of iron oxides was not observed in the alloy samples under the oxide films.

The parameters of the lines of the initial intermetallic phases were used for the decomposition of the spectrum of the oxide film.

3.2 State of iron in the oxide films

The ^{57}Fe CEM spectra of the surface oxide films obtained after different times of corrosion of alloy 1 are presented in Fig. 3. ^{57}Fe transmission spectra of two different stages of corrosion are presented in Figs. 4 and 5. ^{57}Fe transmission spectra of the surface oxide films of alloy 2 at the beginning stage and after long corrosion time are presented in Figs. 6 and 7.

The analyze of spectrum in Fig. 3 at the beginning corrosion stage (15 days, thickness $1.2\ \mu\text{m}$) shows the presence of Fe^{3+} and Fe^{2+} ions and the intermetallic compound $\text{Zr}(\text{Fe},\text{Cr})_2$ in oxide films up to a depth of $\sim 0.3\ \mu\text{m}$. The conversion electrons may monitor a depth of $\sim 0.3\ \mu\text{m}$. The presence of $\text{Zr}(\text{Fe},\text{Cr})_2$ proves that not all particles up to a depth of $0.3\ \mu\text{m}$ are oxidized. The Fe^{3+} and Fe^{2+} ions are identified as their solid solutions in ZrO_2 . With increasing oxide film thickness the lines of $\text{Zr}(\text{Fe},\text{Cr})_2$ disappear and the relative intensity of the Fe^{3+} lines increases.

The analysis of the right part in Fig. 3 shows the presence of hyperfine magnetic splittings. In the thin film (15 days, $1.2\ \mu\text{m}$) they are identified as lines of $\alpha\text{-Fe}$ with solid solution of Cr atoms. That is the reason why the spectrum consists of 3 magnetically split components. In the oxide films of 2.0 and $6.0\ \mu\text{m}$ the lines of $\alpha\text{-Fe}$ are not detected. But the lines of Fe_3O_4 can be identified in these oxide films. This means that the particles of $\alpha\text{-Fe}$ are formed simultaneously with the destruction of the $\text{Zr}(\text{Fe},\text{Cr})_2$ particles and the formation of iron solid solution in ZrO_2 in the beginning stage of corrosion. During corrosion the $\alpha\text{-Fe}$ particles are destroyed especially in layers nearest to the sample surface and in these layers the iron oxide Fe_3O_4 is formed.

The spectra of iron in the total oxide layer for alloy 1 are shown in Figs. 4 and 5. According to [5] iron can be identified in states of $\text{Zr}(\text{Fe},\text{Cr})_2$, Fe_3O_4 , $\alpha\text{-Fe}$ with Cr atoms and the ions Fe^{3+} and Fe^{2+} in solid solutions in ZrO_2 . With increasing oxide film thickness the iron in $\alpha\text{-Fe}$ with Cr atoms decreases and Fe_3O_4 increases. The presence of $\text{Zr}(\text{Fe},\text{Cr})_2$ particles is explained by their removal from the metal together with the oxide. A part of such particles are not oxidized in inner oxide layers.

Comparison of the spectra in Figs. 3, 4 and 5 allows to conclude that $\alpha\text{-Fe}$ is oxidized to Fe_3O_4 in the outer layers during corrosion.

Mössbauer spectra, recorded in transmission geometry, of the mechanically separated oxide from alloy 2 are presented in Fig. 6. It is possible to see the presence of lines with hyperfine magnetic splitting of $\alpha\text{-Fe}$ in this spectrum.

The lines of $\text{Zr}(\text{Fe},\text{Cr})_2$ and lines of Fe^{3+} and Fe^{2+} ions in solid solutions in ZrO_2 are detected clearly.

The spectrum of ^{57}Fe in oxide film obtained at $t = 350\ ^\circ\text{C}$, $p = 16.8\ \text{MPa}$ on alloy 2 (Fig. 7) shows the existence of lines of $\text{Zr}(\text{Fe},\text{Cr})_2$, $\alpha\text{-Fe}$ with Cr atoms, a mixture of $\alpha\text{-Fe}_2\text{O}_3$ and Fe_3O_4 , and Fe^{3+} and Fe^{2+} ions in solid solutions in ZrO_2 . However, these lines have a large linewidth which can be indicative of nonequivalent positions of iron atoms in this phase. The spectra of the oxide films having the same thickness and of the same alloy

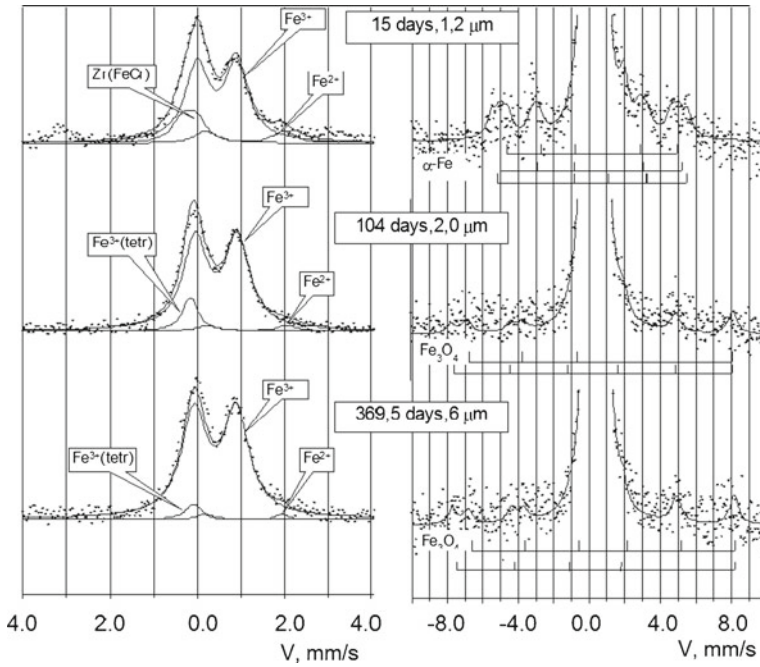


Fig. 3 ^{57}Fe CEM spectra of oxide films of alloy 2 (Zr-1.0 wt%Fe-1.2 wt%Sn-0.5 wt%Cr) with different velocity scale and for different times of the corrosion test

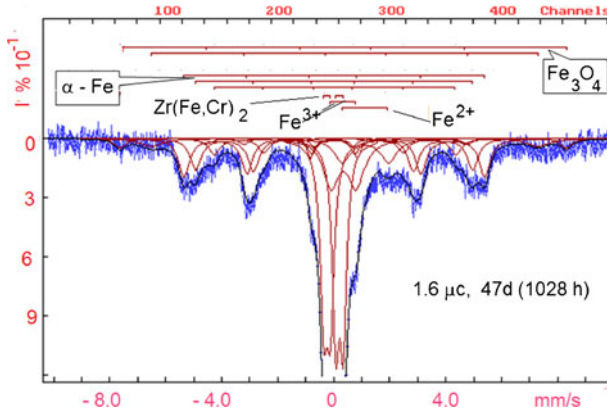


Fig. 4 ^{57}Fe transmission spectrum of the oxide film of alloy 1. The oxide layer was removed mechanically. The spectrum is obtained at room temperature

(2) are represented in Figs. 6 and 7. The difference between these two spectra is the presence of the superposition of lines of $\alpha\text{-Fe}_2\text{O}_3$ and $\alpha\text{-Fe}$ in the spectrum in Fig. 7 (350 °C), while in Fig. 6 (500 °C) only lines of $\alpha\text{-Fe}$ are clearly visible.

Fig. 5 The transmission spectrum of ^{57}Fe of an oxide film of alloy 1. The oxide was removed mechanically. The spectrum is obtained at room temperature

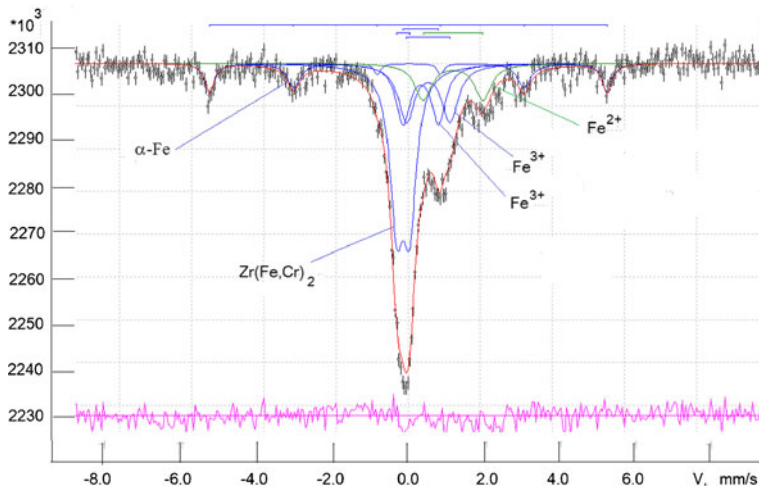
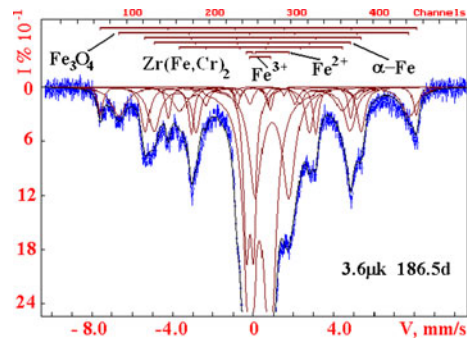


Fig. 6 ^{57}Fe Mössbauer spectra of an oxide film with a thickness of $2.2\ \mu\text{m}$, removed from Zr-1.4 wt%Fe-0.7 wt%Cr (alloy (2)) after 10 h of corrosion ($500\ ^\circ\text{C}$, 10 MPa)

3.3 Change of the state of iron atoms in the oxides as a function of temperature

For the determination of the nanoparticle size of iron oxide particles one oxide sample is investigated at two temperatures. The obtained spectra are shown in Fig. 8. The broadening of these lines is probably associated with the superposition of several systems with magnetic hyperfine splitting. These systems correspond to different iron oxide phases. In the case of $\alpha\text{-Fe}$ metallic particles the dissolution of Cr atoms decreases the magnitude of hyperfine magnetic splitting. Such phenomena have been observed before [6]. In such case the spectra of alloys with iron and chrome atoms ($\alpha\text{-Fe}(\text{Cr})$ chromium steel) have been fitted well by a superposition of five hyperfine magnetic splittings. We used this model to fit the spectrum of chrome-containing $\alpha\text{-Fe}$ particles in oxide film (Fig. 8).

The positions of the outer peaks (1 and 6) in the spectrum coincide with one of the lines of $\alpha\text{-Fe}_2\text{O}_3$ or Fe_3O_4 oxide compounds. Besides, the corrosion process of ZrFeCr intermetallic particles [5] leads to the formation of $\alpha\text{-Fe}_2\text{O}_3$ with inclusions of Cr atoms. Additional atoms in crystal structure of $\alpha\text{-Fe}_2\text{O}_3$ (as well as with Co atoms [6]) should lead to additional superposition of hyperfine magnetic splittings. Non-stoichiometry of $\alpha\text{-Fe}_2\text{O}_3$

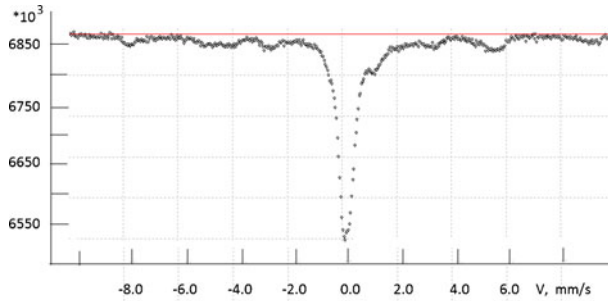


Fig. 7 ^{57}Fe Mössbauer spectra of an oxide film with a thickness of $2.2\ \mu\text{m}$, removed from Zr-1.4 wt%Fe-0.7 wt%Cr (alloy (2)) after 4650 h of corrosion ($350\ ^\circ\text{C}$, $16.8\ \text{MPa}$)

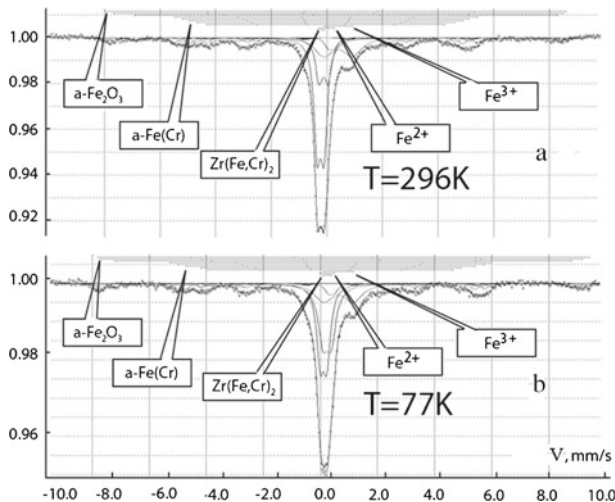


Fig. 8 Transmission ^{57}Fe Mössbauer spectra of an oxide film with a thickness of $14.0\ \mu\text{m}$, removed from Zr-1.4 wt%Fe-0.7 wt%Cr alloy (2) after 2390 h of the corrosion test

and Fe_3O_4 compounds also should lead to a distortion of lines in the spectrum [6–11]. So the fitting of a spectrum that represent a superposition of several magnetic hyperfine splittings is always a difficult task. In this work the weak intensity of some lines also presents some difficulty. Figure 8 shows the presence of several magnetically split components with broad lines.

As difference between alloys 1 and 2 it can be seen that the presence of the lines of $\alpha\text{-Fe}_2\text{O}_3$ are not detected in oxide films of alloy 1. This may be caused by the difference in the corrosion environment (presence of B and Li in water in the case of alloy 1) or by presence of tin in alloy 1.

In order to obtain additional information the spectrum of oxide film was measured also at the temperature of liquid nitrogen (Fig. 8b). The complexity of the lines in the spectrum has essentially not changed. But a displacement of the magnetic split lines in the spectrum of the oxide phases is observed with decreasing temperature. The result of a previous paper [8] has shown that the 6th line should be considerably displaced towards positive velocities.

Table 1 The characteristics of the oxide particles

T, K	kT, J	KV, J	V volume of particles, m ³	Size of particles, nm
298	4.11E-21	1.9E-20	1.9E-25	5.7
77	1.06E-21	4.9E-21	4.9E-26	3.7
5	6.90E-23	3.2E-22	3.2E-27	1.5

This was observed for massive samples of α -Fe₂O₃ with the Morin's transition, and for fine particles without Morin transition. Such a displacement of the 6th line was observed for a spectrum of Fe₃O₄ compound at liquid nitrogen temperature [9, 12]. It is probable that in the spectrum of the oxide film (Fig. 8) the hyperfine magnetic split lines are caused by a mixture of non-stoichiometric compounds of α -Fe₂O₃ and Fe₃O₄. Moreover, Mössbauer investigations of corrosion processes in iron containing materials with deficiency of oxygen atoms often show the presence of a mixture of these oxide compounds.

In our investigation the spectra with hyperfine magnetic splitting larger than for α -Fe were fitted using spectra parameters of iron oxide compounds.

The α -Fe₂O₃, Fe₃O₄ compounds have close values of resonant absorption probability. Therefore the area of the lines in the spectra of these oxide phases can be considered to be proportional to the concentration of iron atoms in these oxides. The analysis shows that the total area of the spectrum lines of α -Fe₂O₃ and Fe₃O₄ compounds with decreasing temperature increases more than the resonant absorption probability changes. This means the fraction of iron atoms in magnetic phases has increased. Such increase can be explained by the presence of oxide particles (α -Fe₂O₃ and Fe₃O₄) with a size of 10 nanometers. Such particles change from their superparamagnetic to a ferromagnetic state at 78 K. This results in an increasing area of the spectrum with magnetic hyperfine splitting.

A measurement at liquid helium temperature (5 K) shows that a further slight increase of the area under the lines of the oxide compounds α -Fe₂O₃ and Fe₃O₄ can be noticed with respect to the increase of the resonant absorption probability. This fact can also be associated with a fraction of the particles passing for the superparamagnetic phase to the ferromagnetic phase (5K–78K). The quantity of iron in small size precipitates is small and this is why there is no appreciable increase of the oxide fractions in magnetic states

The method to estimate the particle size of the particles passing from the superparamagnetic to the ferromagnetic state was given in papers [8, 10, 13]. The formula $t=t_0 \exp(KV/kT)$ was used, where V = volume of particle, k = Boltzmann constant, T = temperature. The values of K, the effective anisotropy constant, were estimated in these papers for oxide phases. Using these values we have made calculations for 3 different temperatures. The average size of the particles are listed in the Table 1.

The data of this table show the possible sizes of oxide nanoparticles that are present in oxide film of zirconium alloys formed during corrosion process.

4 Conclusions

Mössbauer investigations of oxide films formed on samples of zirconium alloys Zr-1.0 wt%Fe-1.2 wt%Sn-0.5 wt%Cr and Zr-1.4 wt%Fe-0.7 wt%Cr subjected to corrosion in a steam-water environment were carried out. It is shown that the corrosion process has an effect on the intermetallic particles Zr(Fe_{1-x}, Cr_x)₂ of the zirconium alloy and leads

to the formation of metallic phases α -Fe and iron oxide compounds containing iron and chromium. Part of the oxide compounds may be in form of nanoparticles.

The valence state of iron atoms in oxide films depends on the corrosion environment. During corrosion tests in oxygen environment the high water temperature and pressure increase the quantity of α -Fe₂O₃; the presence of B and Li increases the probability of the formation of Fe₃O₄.

The results of the present work invite to pay attention to the presence of oxide inclusions with small sizes during microscopic investigations of oxide films of zirconium alloys.

Acknowledgment This research was supported by the Ministry of education and science of the Russian Federation and with partially using the equipment of the center "Hetero structural microwave electronics and wideband semiconductor physics".

References

1. Pecheur, D., Filippov, V.P., Bateev, F.B., Ivanov, Y.Y.: Mössbauer investigations of the chemical states of tin and iron atoms in zirconium alloy oxide film zirconium. In: Moan, C.D. (ed.) The Nuclear Industry 13 International Symposium ASTM STR 1423, pp. 135-153. ASTM International, PA (2002)
2. Sawicki, J.A.: Iron-bearing precipitates in Zircalloys: a Mössbauer spectroscopy study. *JNM* **228**, 238–247 (1996)
3. Bozzano, P.B., Ramos, C., Saporiti, F., Vazquez, P.A., Versaci, R.A., Saragovi, C.: Oxidation of the hexagonal Zr(Cr_{0.4}, Fe_{0.6})₂ Laves phase. *JNM* **328**, 225–231 (2008)
4. Filippov, V.P., Shikanova, Y.A.: Conversion of intermetallic compounds in zirconium alloys at room temperature. *Fizika I Khimiya Obrabotki Materialov (Phys. Chem. Mater. Process.) (rus)*, **1**, 90–91 (2004)
5. Filippov, V.P., Petrov, V.I., Lauer, D.E., Shikanova, Y.A.: Mössbauer investigations of corrosion environment influence on fe valence states in oxide films of zirconium alloys. *Hyperfine. Interact.* **168**, 965–971 (2006)
6. Boiko, N.V., Devyatko, Y.N., Evstyukhina, I.A.: Investigation of fine atomic structure of low-activation chromium steel using Mössbauer spectroscopy and calorimetry within the temperature range of ductile-to-brittle transition. *Inorg. Mater. Appl. Res.* **3**(2), 102–106 (2012)
7. Sun, K., Lin, M.X., He, T., Luo, H.L.: The Mössbauer study of α -Fe₂O₃ fine particles with and without absorber cobalt. *Phys. Stat. Sol. (a)* **115**(2), 539–546 (1989)
8. Kundig, W., Bommel, H., Constabaris, G., Lindquist, R.H.: Some properties of supported small α -Fe₂O₃ particles determined with Mössbauer effect. *Phys. Rev.* **142**(2), 327–333 (1966)
9. Krupyansky, Y.F., Suzdalev, I.P.: Size effect in small Fe₃O₄ particles. *JETP* **41**(8), 736–742 (1975)
10. Roggwiller, K.W.: Mössbauer spectra of superparamagnetic Fe₃O₄. *Solid State Commun.* **12**, 901–903 (1973)
11. Senn, M.S., Wright, J.P., Attfield, J.P.: Charge order and three-site distortions in the Verwey structure of magnetite. *Nature* **481**(12), 173–176 (2012)
12. Jackson, M., Moskowitz, B., Bowles, J.: Interpretation of Low-Temperature Data Part III: The Magnetite Verwey Transition (Part A), vol. 20, no. 4, pp. 1-12. The IRM Quarterly University of Minnesota (2011)
13. Mørup, S., Frandsen, C., Hansen, M.F.: Uniform excitations in magnetic nanoparticles. *J. Nanotechnol.* **1**, 48–54 (2010)